Changes in the Shape and Mobility of Colloidal Gold Nanorods with Electrospray and Differential Mobility Analyzer Methods

ARTICLE *in* LANGMUIR · DECEMBER 2005

Impact Factor: 4.46 · DOI: 10.1021/la0513196 · Source: PubMed

5 AUTHORS, INCLUDING:

Dong Keun Song
Korea Institute of Machinery and Materials
21 PUBLICATIONS **72** CITATIONS
SEE PROFILE

Wuled Lenggoro
Tokyo University of Agriculture and Technology
122 PUBLICATIONS **3,229** CITATIONS
SEE PROFILE

Sang Soo Kim
Korea Advanced Institute of Science and Tec…
168 PUBLICATIONS **2,025** CITATIONS
SEE PROFILE

Changes in the Shape and Mobility of Colloidal Gold Nanorods with Electrospray and Differential Mobility Analyzer Methods

Dong Keun Song,[†,‡] I. Wuled Lenggoro,[†] Yoshimasa Hayashi,[§] Kikuo Okuyama,*[,†] and Sang Soo Kim[‡]

Department of Chemical Engineering, Graduate School of Engineering, Hiroshima University, 1-4-1 Kagamiyama, Higashi-Hiroshima-shi, Hiroshima 739-8527, Japan, Aerosol & Particle Technology Laboratory, Department of Mechanical Engineering, Korea Advanced Institute of Science and Technology, Guseong-dong, Yuseong-gu, Daejeon 305-701, Korea, and Hiroshima Joint Research Center for Nanotechnology Particle Project, Japan Chemical Innovation Institute, 1-3-1 Kagamiyama, Higashi-Hiroshima-shi, Hiroshima 739-8530, Japan

Received May 17, 2005. In Final Form: August 11, 2005

The potential of the electrospray technique in analyzing the structure of nonspherical colloidal particles that are below 100 nm in volume-equivalent diameter was demonstrated by online size measurement using a differential mobility analyzer (DMA) with a condensation nucleus counter (CNC) system. The measured mobility of gold nanorods was confirmed by electron microscope images and the theoretical calculation of particle mobility using the dynamic shape factor and slip correction factor. To evaluate the mobility, rod particles were modeled as both a cylinder and a prolate spheroid. This study also showed that the organic surfactant coated on rod particles might be removed and that the rod particles became spherical upon the elevation of the ambient temperature during the gas-phase dispersion of colloidal nanoparticles. Moreover, the thickness of the surfactants coated on rod particles was estimated by comparing the theoretically and experimentally obtained mobilities.

Introduction

The advancement of miniaturization in the microelectronics industry and nanoscale fabrication using conventional techniques has lower size limits because of technical and economic factors. This has redirected research and development efforts toward approaches in which chemical techniques are used in the fabrication of functional nanostructures, namely, tubes, cylinders, and wires, with the ultimate aim of producing hierarchical structures capable of performing sophisticated functions.

It is well-known that a wide variety of liquid-phase methods using chemical approaches such as microemulsions, sol−gel, and reverse micelles are available for producing colloidal nanoparticles. They are also frequently used in studies related to materials science, chemistry, and biology, including macromolecules, sols, nanocrystallites, dendrimers, polymer latexes, and proteins or living cells. Detailed information on nanoparticle size and dispersity is highly desirable because many of the properties associated with nanosized particles are strongly size dependent. Moreover, information on the structure or the aspect ratio is also essential for nonspherical functional structures such as gold nanorods. Gold nanorods can be used in applications such as optical filters and heat-ray cut filters.

To analyze the structure of colloidal nanoparticles, microscopy techniques such as transmission or scanning electron microscopy (TEM/SEM), scanning near-field optical microscopy,[1] scanning probe microscopy, and atomic force microscopy have conventionally been used.[2] In these methods, good sampling techniques and skilled operation, as well as time-consuming procedures, are required. Schmid and Chi[3] reported that for a smaller order, the imaging or sizing of metallic Au clusters by high resolution TEM is usually accompanied by a coalescence process between the cluster molecules, leading to colloidal nanoparticles of a larger size in seconds. Lenggoro et al.[4] proposed an online technique for measuring the size distribution of colloidal particles. The procedure involves (1) transferring the colloidal particles from the liquid to the gas phase (as an aerosol) using electrospray and (2) particle sizing in the gas phase using a differential mobility analyzer (DMA). In the measurement system consisting of an electrospray and a DMA, the size distributions of particles are measured as their electrical mobility distribution.

It is well-known that the shape and size of a particle greatly influence its properties (optical, electrical, mechanical, etc.); therefore, it is important to obtain information on the shape and size distribution from the measured mobility distribution. When particles are suspended in a fluid, the drag force on a nonspherical particle is generally greater than that on a sphere of the same volume moving with the same velocity. The dynamic shape factor and the slip correction factor are two important parameters for determining fluid drag on nonspherical particles. The dynamic shape factor of nonspherical particles depends on the particle size, shape, and orienta-

* Corresponding author. E-mail: okuyama@hiroshima-u.ac.jp.
† Hiroshima University.
‡ Korea Advanced Institute of Science and Technology.
§ Japan Chemical Innovation Institute.

(1) Zenobi, R.; Deckert, V. *Angew. Chem., Int. Ed.* **2000**, *39*, 1746−1756.
(2) Lacava, L. M.; Lacava, B. M.; Azevedo, R. B.; Lacava, Z. G. M.; Buske, N.; Tronconi, A. L.; Morais, P. C. *J. Magn. Magn. Mater*. **2001**, *225*, 79−83.
(3) Schmid, G.; Chi, L. F. *Adv. Mater.* **1998**, *10*, 515−526.
(4) Lenggoro, I. W.; Xia, B.; Okuyama, K.; de la Mora, J. F. *Langmuir* **2002**, *18*, 4584−4591.

10.1021/la0513196 CCC: $30.25
Published on Web 10/07/2005

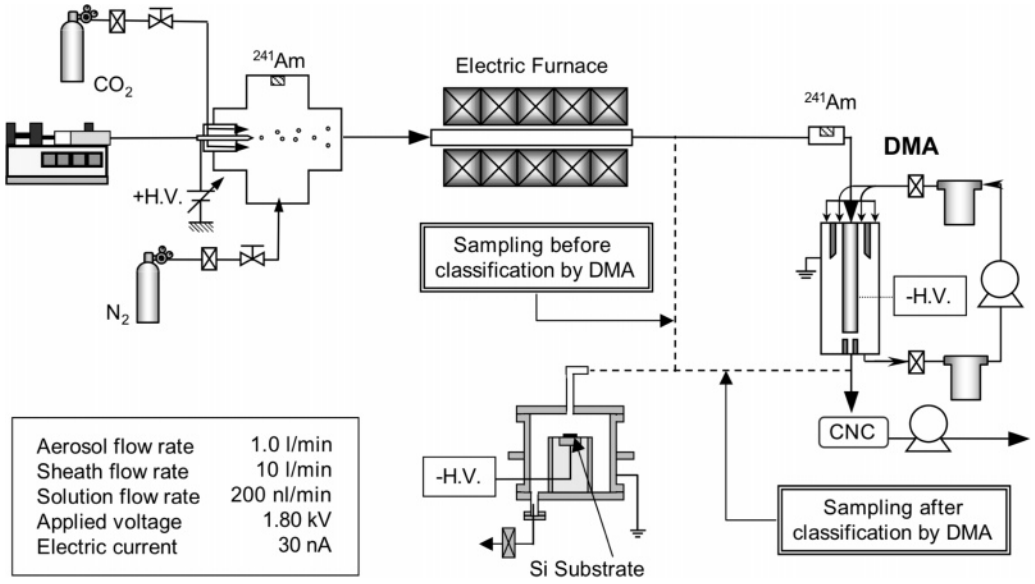

Figure 1. Schematics of the experimental setup.

tion, and the particle flow regime. The slip correction factor is also used to determine the effect of slip in the transition regime compared to the continuum regime.

In this study, electrospray was used to transfer the colloidal gold nanorod particles to the gas phase, which was followed by "in-flight" heating. After this heating process, the shape and size of the particles were observed by both TEM/SEM images and mobility measurements using a DMA. Changes in the shapes and the mobilities of the particles were observed as the heating temperature of the electric furnace changed, and these changes were confirmed by TEM/SEM images and mobility measurements using the DMA. The effects of the surfactants surrounding the nanoparticles on their measured mobilities were investigated by a theoretical mobility calculation for nonspherical particles.

Experimental Methods

As shown in Figure 1, the system used for the online sizing measurements, which was similar to that reported by Lenggoro et al.,[4] consisted of (1) a homemade electrospray source, (2) a neutralizer (Am-241), (3) a tubular electric furnace (inner diameter: 15 mm; length: 200 mm), and (4) a size-analysis section, including a DMA (Model 3085, TSI Incorporation, Shoreview, MN) and a particle counter (a condensational particle/nucleus counter (CNC), TSI model CNC 3025) operated under atmospheric pressure. The gold nanorod particles were supplied by Mitsubishi Materials Corp. and Dai Nippon Toryo Co., Ltd. and were prepared according to the improved process of rapid synthesis, which combines chemical reduction with photoirradiation.[5] The gold nanorod particles were coated by organic compounds (mainly hexadecyltrimethylammonium bromide, C_{16}TMABr) to prevent particle agglomeration. The gold nanorod particles were dispersed in a mixture of toluene/ethanol, and small droplets containing gold rod particles were generated by an electrospray in the cone-jet mode. The volumetric flow rates of the solution and carrier gas (N_2/CO_2 = 90:10, in volume %) used in the electrospray were 0.2×10^{-6} L/min and 1.0 L/min, respectively. The generated droplets were fed into a tubular electric furnace and heated. The temperature of the electric furnace was varied from room temperature (25 °C) to 800 °C and controlled by three temperature controllers and thermocouples. The temperature profile along the tubular furnace was independently monitored by a thermocouple. The particles heated in the electric furnace were sampled (using an SEM/TEM grid) in the outlet of the furnace to investigate the changes in shape. The mobility of the particles was measured by a DMA−CNC system and also sampled using the SEM/TEM grid after the mobility was measured. The DMA dimensions are listed in Table 1.

(5) Niidome, Y.; Nishioka, K.; Kawasaki, H.; Yamada, S. *Chem. Commun.* **2003**, 2376−2377.

Table 1. DMA Dimensions

inner radius (r_i)	9.37 ± 0.01 mm
outer radius (r_o)	19.61 ± 0.01 mm
length (L)	49.87 ± 0.15 mm
aerosol flow rate (Q_a)	1 L/min
sheath flow rate (Q_c)	10 L/min

Theoretical Considerations

Electrical Mobility of Nonspherical Particles. The charged particles in the concentric annulus of a DMA are moved downstream by sheath flow and accelerated to the inner electrode by an electrostatic field. The particles passing through the sampling slit of the inner electrode have an electrical mobility (Z_p) with a narrow bandwidth (ΔZ_p). The electrostatic force acting on a particle having a charge q in an electric field of strength E is $F_{elec} = qE$. The equation of motion for a particle of charge q moving at velocity v in a fluid with velocity u in the presence of an electric field of strength E is

$$m_p \frac{dv}{dt} = qE - (u - v) f_d(\theta) \quad (1)$$

in which m_p is the mass of the particle, θ is the angle between the major axis of the particle and the direction of particle motion, and $f_d(\theta)$ is the drag coefficient defined by $f_d(\theta) = F_d(\theta)/(u - v)$. At steady state in the absence of a background fluid velocity, the particle velocity is such that the electrical force is balanced by the drag force and

$$f_d(\theta) v_e = qE \quad (2)$$

in which v_e is termed the electrical migration velocity. The electrical mobility Z_p is defined by $v_e = Z_p E$, therefore

$$Z_p = q/f_d(\theta) \quad (3)$$

For spherical particles of diameter d_p, the drag coefficient $f_d(\theta)$ is independent of the angle between the polar axis and the direction of movement of the particle and becomes $f_{d,sphere} = 3\pi\eta d_p/C_c$, in which η is the viscosity of the fluid.

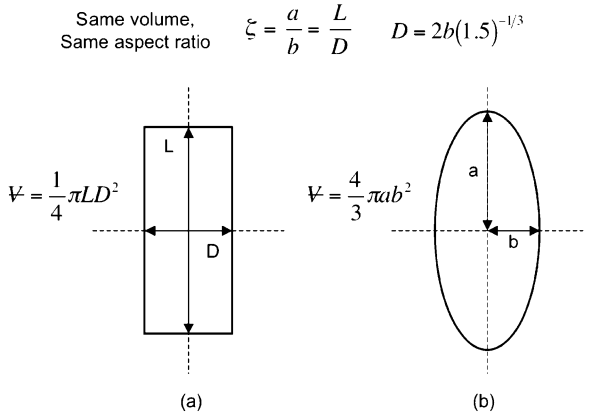

Figure 2. Modeling of rod particles as a cylinder (a) and as a prolate spheroid (b).

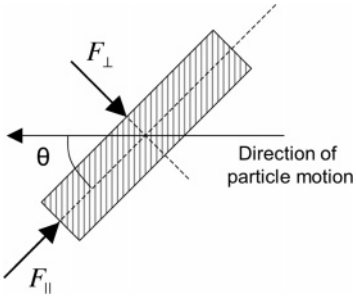

Figure 3. Motion of an elongated particle and its components of drag forces.

Table 2. Mixing Ratio of Liquid-Phase Materials, Measured Peak Mobility, and Number Concentration

case	G1	G2	G3	G4
gold particles (mL)	1	0.1	0.02	0.01
toluene (mL)	0.3	3	3	3
ethanol (mL)	0.2	2	2	2
peak mobility [10^{-8} m^2/(V s)]	1.41	8.14	8.14	8.14
peak concentration (#/cm^3)	30.7×10^3	38.0×10^3	750	313

Dynamic Shape Factor. The fluid drag on a suspended particle determines its velocity and mobility. For nonspherical particles moving at a creeping flow, the drag force can be related to that for a spherical particle of equal volume with the same velocity by[6]

$$F_d = -3\pi\eta d_{ve} v \kappa_0(\theta) \quad (4)$$

in which d_{ve} is the diameter of a sphere with the same volume as the nonspherical particle. This equation is valid in the continuum regime in which the particles are much larger than the mean free path (λ) of the fluid molecules (Kn $\approx$ 0). The aerodynamic behavior of nonspherical particles, especially elongated particles, has been modeled using the theory of prolate spheroids with a low Reynolds number and low Knudsen numbers, and a cylindrical particle has been modeled as a prolate spheroid on the basis of an approximation of the slender-body theory.[6−8] The dynamic shape factor or friction coefficient, $\kappa_0(\theta)$, depends on the orientation of a nonisometric particle with respect to the direction of flow. A substantial database of experimental results for fluid drag has been accumulated for particles with various shapes.[9,10] These measurements

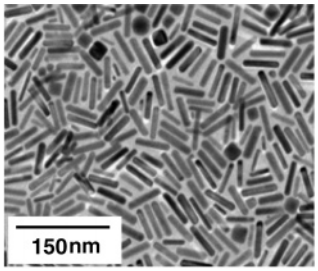

Figure 4. A TEM image of gold nanorod particles.

Table 3. Dimensions of Gold Nanorods, Obtained from TEM Images

length (nm)	73.95 ± 9.67
diameter (nm)	13.00 ± 1.82
aspect ratio (L/D)	5.76 ± 0.93
equivalent-volume diameter (nm)	26.50 ± 3.03

were made with macroscopic bodies in sedimentation tanks filled with viscous fluid. These experiments showed that the drag force and the dynamic shape factor depended on both the aspect ratio of the particle and the orientation of the particle with respect to the flow direction. The experimental values of κ_0 for cylindrical shapes and chain aggregates are available in the literature.[11] The theoretical predictions of κ_0 for spheroids and other shapes have been calculated.[12] The gold nanorods used in this study can be described as either cylinders with flat ends or prolate spheroids (Figure 2). The dynamic shape factor for both a cylinder and a prolate spheroid in the continuum regime is given in the Appendix. At low particle Reynolds numbers ($\ll$0.1), the orientation of aerosol particles is random because of the Brownian motion of particles.[6] In this case, the dynamic shape factor of the particles with rotational symmetry, including spheroids and cylinders, is an average:

$$\frac{1}{\kappa_{ran}} = \frac{1}{3}\left(\frac{1}{\kappa_{||}} + \frac{2}{\kappa_\perp}\right) \quad (5)$$

The subscripts || and $\perp$ indicate that the polar axis of the cylinder is respectively parallel and perpendicular to the direction of particle motion (Figure 3).

Slip Correction Factor and Adjusted Diameter. Between the continuum and free molecular regimes is the transition regime (0 < Kn < 100), in which most aerosol studies are performed. In the transition regime, the Cunningham slip correction factor is used for spherical particles to obtain the correct drag force,

$$F_d = -\frac{3\pi\eta d_p v}{C(d_p)} \quad (6)$$

The slip correction factor has the following expression:

$$C = 1 + \mathrm{Kn}[\alpha + \beta \exp(-\gamma/\mathrm{Kn})] \quad (7)$$

Following the definition of Fuchs,[6] the drag force of nonspherical particles in the transition regime can be expressed as

$$F_d = -\frac{3\pi\eta d_{ve} v \kappa}{C(d_{ve})} \quad (8)$$

in which $C(d_{ve})$ has the same form as that in eq 7, with

(6) Fuchs, N. A. *The Mechanics of Aerosols*; Pergamon: New York, 1964.
(7) Batchelor, G. K. *J. Fluid Mech.* **1970**, *44*, 419−440.
(8) Cox, R. G. *J. Fluid Mech.* **1970**, *44*, 791−810.
(9) Happel, J.; Brenner, H. *Low Reynolds Number Hydodynamics*; Prentice Hall: Englewood Cliffs, New Jersey, 1965.
(10) Kasper, G. *Aerosol Sci. Technol.* **1982**, *1*, 187−200.
(11) Kasper, G. *J. Aerosol Sci.* **1985**, *16*, 535−556.
(12) Dahneke, B. E. *J. Aerosol Sci.* **1973**, *4*, 139−145.

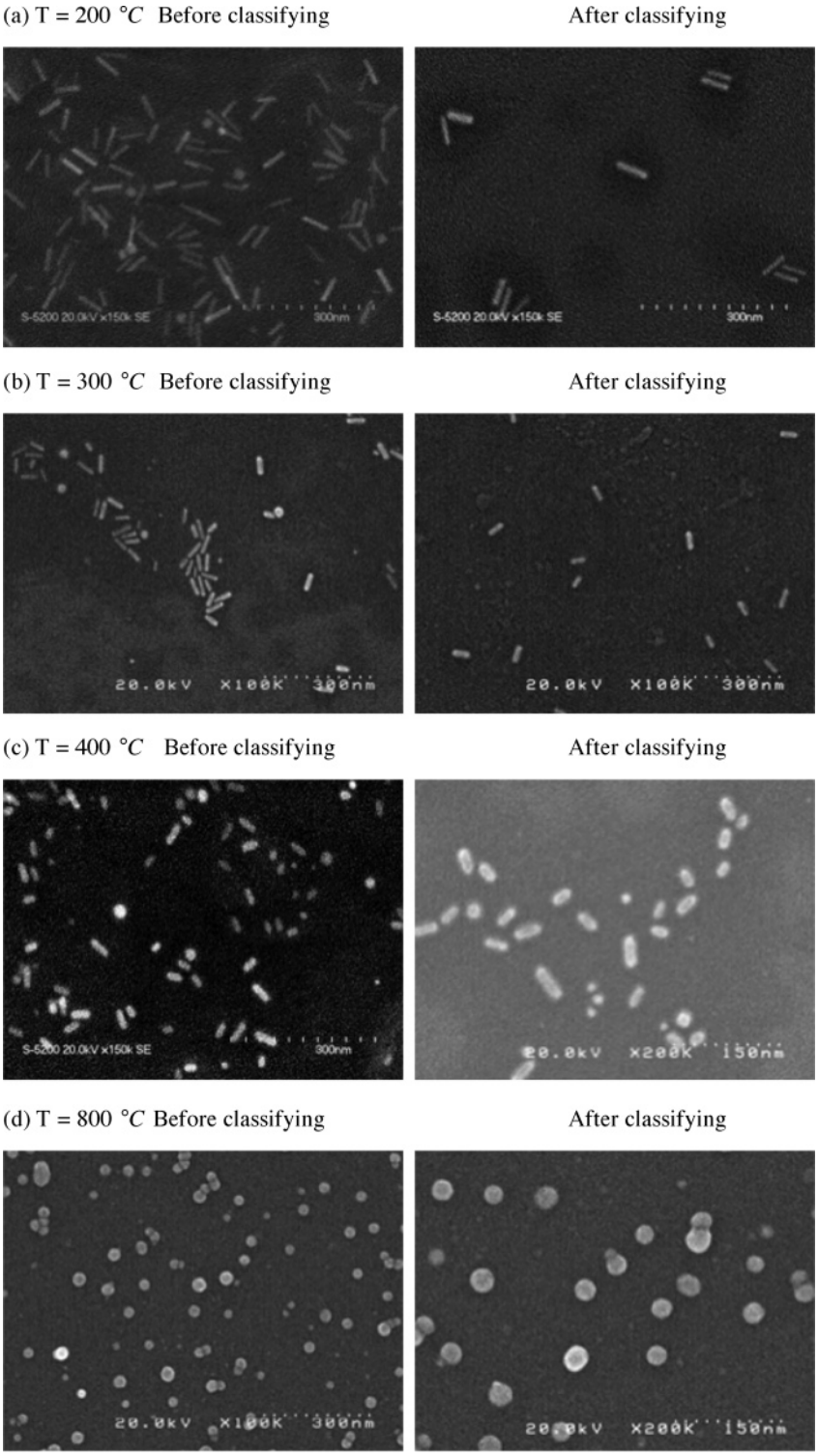

Figure 5. SEM images sampled before and after classification by a DMA.

d_{ve} substituted for d_p. Available data reported in the literature show that κ is not constant ($\kappa = \kappa_0$), but is instead a function of the Knudsen number if the measured drag force is expressed by eq 8.[13−16] Dahneke[17] proposed an adjusted sphere diameter, d_a, which gives the same drag force in the free molecular regime as the particle in question:

$$F_d = -\frac{3\pi\eta d_{ve} v \kappa_0(\theta)}{C(d_a)} \tag{9}$$

The drag force of a nonspherical particle in the free molecular regime can be obtained from the asymptotic form of Stoke's law for Kn > 100,

$$F_d = -\frac{3\pi\eta d_{ve} v \kappa_0(\theta)}{(2\lambda/d_a)(\alpha+\beta)} \tag{10}$$

(13) Horvath, H. *J. Aerosol Sci.* **1979**, *10*, 309−315.
(14) Allen, M. D.; Raabe, O. G. *J. Aerosol Sci.* **1985**, *16*, 57−67.
(15) Cheng, Y.-S.; Allen, M. D.; Gallegos, D. P.; Yeh, H.-C.; Peterson, K. *Aerosol Sci. Technol.* **1988**, *8*, 199−214.
(16) Cheng, Y.-S.; Yeh, H.-C.; Allen, M. D. *Aerosol Sci. Technol.* **1988**, *8*, 109−123.
(17) Dahneke, B. E. *J. Aerosol Sci.* **1973**, *4*, 163−170.

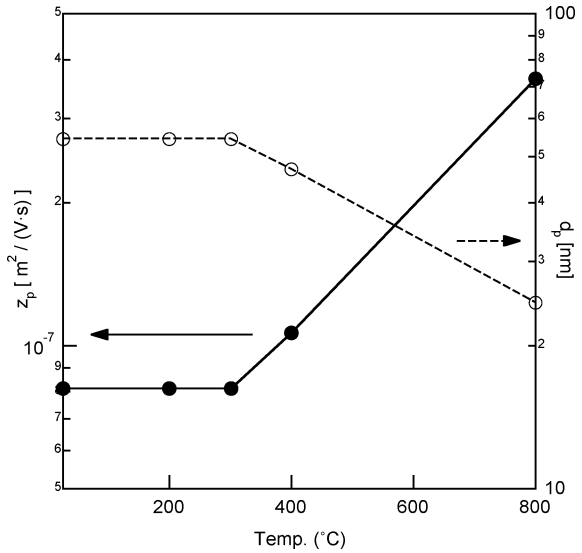

Figure 6. Measured peak mobility and its corresponding sphere diameter.

By equating eqs 9 and 10, we can obtain the adjusted sphere diameter of the spheroid and the cylinder particle. With the volume-equivalent diameter of the cylinder and spheroid, the mobility of nonspherical particles can be obtained using eq 3 and the drag coefficient given by

$$f_d(\xi,\theta) = -\frac{3\pi\eta d_{ve}\kappa_0(\theta)}{C(d_a)} \quad (11)$$

in which the slip correction factor is given by[14]

$$C(d_a) = 1 + (2\lambda/d_a)\{1.142 + 0.558\exp[-0.999(d_a/2\lambda)]\} \quad (12)$$

Results and Discussion

To size colloidal particles, it is important to make droplets with one particle inside, and to generate enough droplets to be measured by the DMA−CNC system. The number of particles contained in a droplet generated by an electrospray system varied according to the concentration of the liquid-phase material. To investigate the number of particles in a droplet and the number concentration of the generated droplets, the volumetric mixing ratio of aqueous gold particles, toluene, and ethanol was varied, and the mobility distribution of particles was measured by the DMA−CNC system. The mixing ratios of the gold nanorod particles, toluene, and ethanol and the measured mobility and peak number concentration of particles are listed in Table 2. For G1, the measured mobility of particles was lower than that for G2, G3, and G4. The measured mobilities had the same values when the concentration of gold particles was lower than that for G2, meaning that the generated droplets for G2, G3, and G4 only had one particle inside.

The shapes and mobilities of the heated rod particles were observed by both a sampling SEM grid and measurement using the DMA−CNC system. Figure 4 shows the SEM images of the rod particles imbedded in a liquid solution. The statistical information for the dimensions (length, diameter, aspect ratio, and volume-equivalent diameter) of the rod particles was measured from Figure 4 and is listed in Table 3. Figure 5 shows SEM images of the sampled particles before and after classification by a DMA at designated electric furnace heating temperatures (from 200 °C to 800 °C). The shapes of the rod particles began to change and become spheroid-like at temperatures of 400 °C or higher. Furthermore, the particles became almost spherical at 800 °C. Although the heating temperature was lower than the melting temperature of gold, the shape of the gold particles was altered because the melting temperature of nanoparticles is size dependent and lower than the bulk melting temperature.[18] The surfactant (C_{16}TMABr) coated on the nanorods was not removed below an electric furnace heating temperature of 400 °C. This organic surfactant began to be removed at heating temperatures of 400 °C and higher. Lee and Liu[19] reported the thermal properties of C_{16}TMABr as a surfactant for the synthesis of a vanadium−aluminum system. They used thermogravimetric (TG) analysis and differential thermal analysis (DTA) and found that there is a weight loss between 150 and 450 °C that is accompanied by exothermic peaks, indicating the decomposition of C_{16}TMABr in air. Thermal analysis of the surfactant (without gold nanorods) was also performed using TG/DTA in our laboratory and showed the same results as Lee and Liu reported. It should be noted that there is a difference in heating time or heating rate between the conventional TG/DTA and the present in-flight heating technique. The heating rate of TG/DTA is 10 °C/min; that is, 40 min are necessary for 400 °C. On the other hand, in the case of in-flight heating, the total heating time (residence time of the aerosol in the furnace) is only a second.

The mobility of heated droplets was measured by a DMA−CNC system. From room temperature to 300 °C, there was no change in the measured mobility. However, as the temperature of the electric furnace increased, the measured mobility decreased, as shown in Figure 6. At 800 °C, we found that the particles were almost spherical and that the particle size diameter that was converted from the measured mobility using the DMA−CNC system fit well with the diameter measured from the SEM image (Figure 7). Moreover, the mean diameter of the spherical particles agreed with the volume-equivalent diameter of the rod particles.

To observe the effects of the particle shapes, we calculated the electrical mobility of the rod particles using the dynamic shape factor and the slip correction factor in the transition regime. The rod particles were modeled as either cylinders or prolate spheroids, and the adjusted diameters of the rod particles, depending on the direction of motion, were obtained in nanometer size ranges. Finally, the resulting electrical mobility of the rod particles was obtained by eq 3 with a slip correction factor using the calculated adjusted diameter. Figure 8 shows a comparison of the dynamic shape factors for different models and the experimental values for cylinders available from the literature[11] in the continuum regime. Because the theoretical drag force for the cylinder was derived from the slender-body theory, the dynamic shape factor obtained by eq A-6 (Appendix) is much different from the values for the prolate spheroid and the experiment values when the aspect ratio is lower than 3. However, the cylinder model is more suitable than is the spheroid model for aspect ratios in the range from 3 to 15.

The theoretically calculated mobilities of the rod particles varied with the orientation angle of the rod particles and had a minimum value when the rod particles

(18) Couchman, P. R.; Jesser, W. A. *Nature* **1977**, *269*, 481−483.
(19) Lee, D.-S.; Liu, T.-K. *J. Sol.-Gel Sci. Technol.* **2002**, *23*, 15−25.

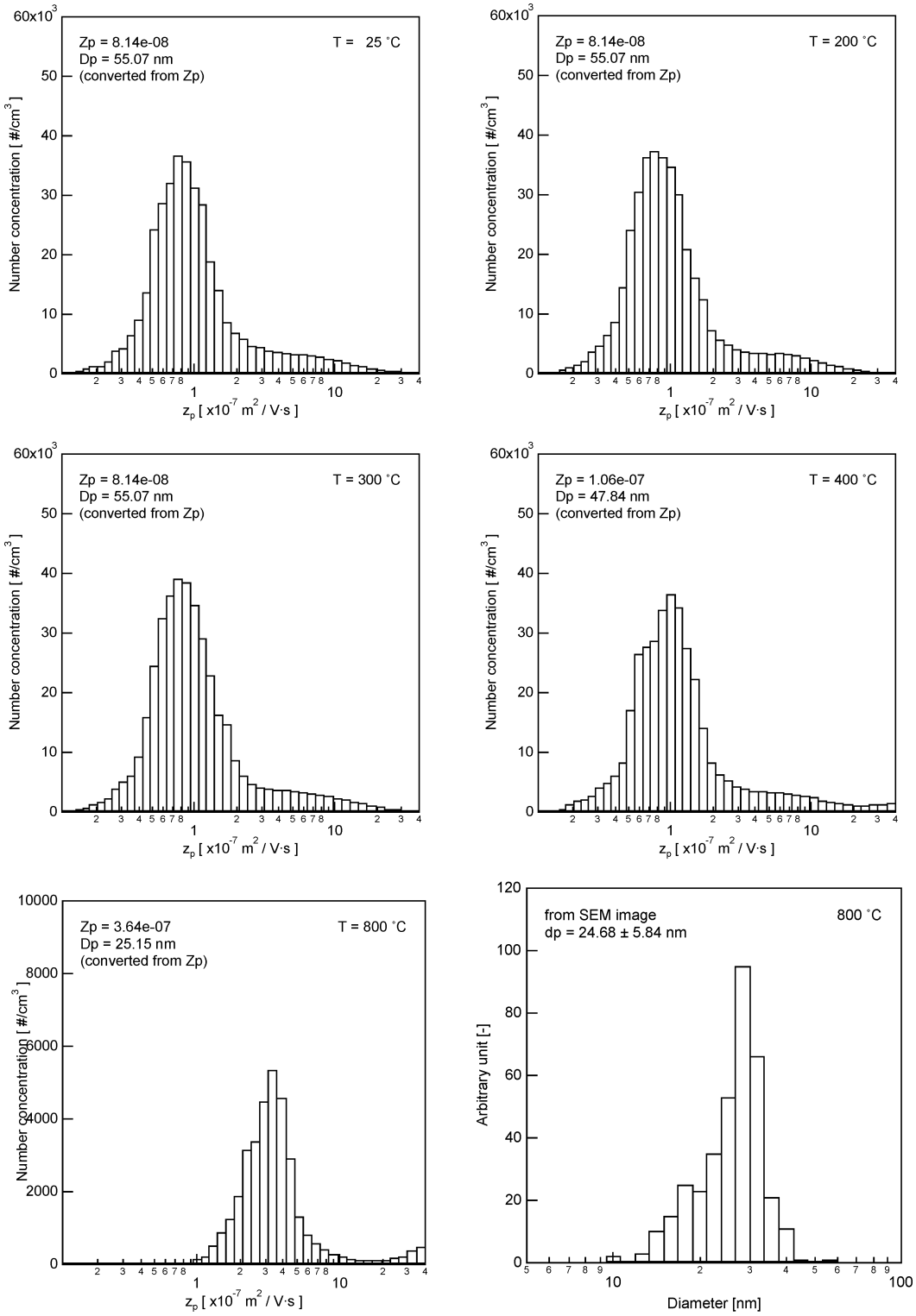

Figure 7. Mobility distribution measured by a DMA and the size data from an SEM image.

moved in a perpendicular direction to the polar axis of the rod particles. Because Brownian motion is dominant, it can be assumed that the rod particles move in a random orientation rather than in a fixed orientation for nanoparticles smaller than 100 nm. The mobility of the particles with random orientation was obtained by averaging the mobility values for particles moving in the directions of the polar and equatorial axes of a rod particle.

On the basis of the dimensions of rod particles measured from the TEM image (Figure 4), the mobility of the rod particles was calculated using theory and compared with the mobility measured by the DMA−CNC system. There were significant differences between the mobility measured by the DMA−CNC system and the theoretical mobility values for spheroids and cylinders. The mobility of the rod particles having a surfactant (C_{16}TMABr) shell thickness δ was calculated to check for the presence of a surfactant shell. On the basis of the assumption that the thickness of the surfactant shell is the same for the polar and equatorial axes, the changes in mobility with changes in δ are shown in Figure 9. Provided that the rod particles were covered by surfactants with a thickness of 7−9 nm,

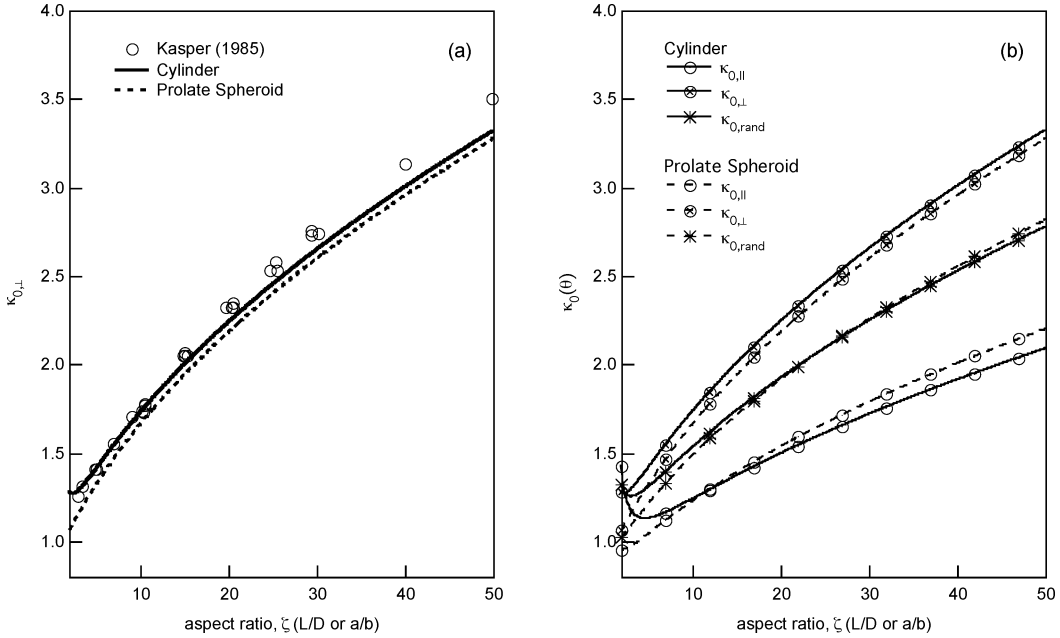

Figure 8. Comparison of the dynamic shape factors for a cylinder and a prolate spheroid and the experimental values.

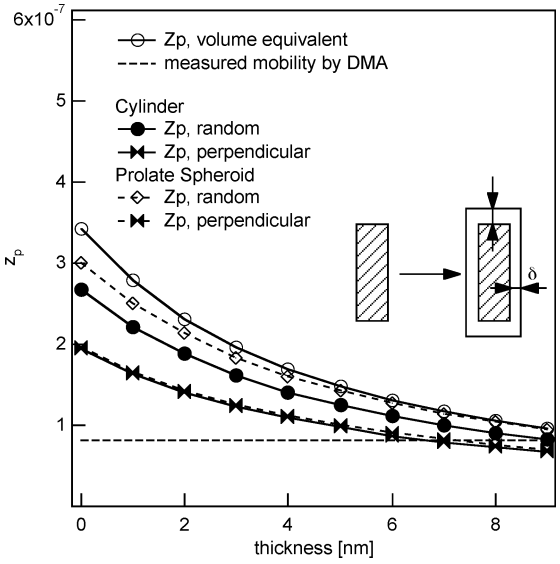

Figure 9. Changes in the mobility of the rod particles with an increase in surfactant thickness.

the mobility for the perpendicular and random orientation fit the measured mobility of the particles well. More over, the differences in the mobility values for perpendicular and random orientations decreased with an increased thickness because the aspect ratio decreased. From the comparison of the mobilities of rod particles having a surfactant shell, we found that the organic surfactant was partially removed at a temperature of 400 °C, and completely removed at a temperature of 800 °C.

Conclusion

The potential of the electrospray technique in analyzing the structure of colloidal nonspherical particles below 100 nm in volume-equivalent diameter was demonstrated by online size measurement using a DMA−CNC and was confirmed by electron microscope (TEM/SEM) images and the theoretical calculation of particle mobility using the dynamic shape factor and the slip correction factor. This study showed that the organic surfactant coated on the rod particles could be partially removed, and a rod-shaped particle could be changed to a sphere by elevating the temperature of the electric furnace. Moreover, the thickness of the surfactants coated on the rod particles was estimated by comparing theoretically and experimentally obtained mobilities.

Acknowledgment. The authors wish thank to Masashi Miyake (Hiroshima University) for his assistance in experiments, Hiroki Hirata (Central Research Institute, Mitsubishi Materials Corp.) and Daigou Mizoguchi (Dai Nippon Toryo Co., Ltd.) for providing valuable discussions on gold nanorods, and Juan Fernandez de la Mora (Yale University) for introducing us to the "stable" electrospray. Grants-in-aid sponsored by the Ministry of Education, Culture, Sports, Science and Technology of Japan, as well as the NEDO-Nanotechnology Particle Project of the Nanotechnology Program provided by the Ministry of Economy, Trade and Industry of Japan, are gratefully acknowledged.

Appendix

Dynamic Shape Factors of a Cylinder and a Prolate Spheroid. The gold nanorods used in this study were in the shape of either a cylinder with flat ends or a prolate spheroid (Figure 2). For prolate spheroid particles with a polar semiaxis (half-length) a and an equatorial semiaxis (radius) b, the dynamic shape factor in the continuum regime is given by

$$\kappa_{0,\text{spheroid}}(\theta) = \frac{\zeta^{2/3}}{3}\left\{\frac{8\psi^2 \sin^2\theta}{[(2\psi^2-1)/\psi]\zeta \ln(\zeta+\psi)+\zeta^2} + \frac{4\psi^2\cos^2\theta}{[(2\psi^2+1)/\psi]\zeta\ln(\zeta+\psi)-\zeta^2}\right\} \quad \text{(A-1)}$$

in which $\psi = \sqrt{\zeta^2-1}$, $\zeta = a/b$, and $d_{ve} = 2b\zeta^{1/3}$. For cylinders of length L and diameter D, the dynamic shape

factor in the continuum regime is

$$\kappa_{0,\parallel} = \left(\frac{2}{3}\right)^{4/3} \zeta^{2/3}\left(\frac{\epsilon + 0.307\epsilon^2}{1 - \epsilon/2} + 0.426\epsilon^3\right) \quad \text{(A-2)}$$

$$\kappa_{0,\perp} = 2\left(\frac{2}{3}\right)^{4/3} \zeta^{2/3}\left(\frac{\epsilon + 0.307\epsilon^2}{1 + \epsilon/2} + 0.119\epsilon^3\right) \quad \text{(A-3)}$$

in which $\zeta = a/b$, $d_{ve} = D(3\zeta/2)^{1/3}$, and $\epsilon = 1/\ln(2\zeta)$. The subscripts $\parallel$ and $\perp$ indicate that the polar axis of the cylinder is respectively parallel and perpendicular to the direction of particle motion (Figure 3). The dynamic shape factor at an arbitrary angle of orientation, θ, is calculated using the formula given by Happel et al.:[9]

$$\frac{1}{\kappa_0(\theta)} = \frac{1}{\kappa_{\parallel}} + \left(\frac{1}{\kappa_{\perp}} - \frac{1}{\kappa_{\parallel}}\right)\sin^2\theta \quad \text{(A-4)}$$

At low particle Reynolds numbers ($\ll$0.1), the orientation of aerosol particles is random because of the Brownian motion of particles.[6] In this case, the dynamic shape factor of particles with rotational symmetry, including spheroids and cylinders, is an average:

$$\frac{1}{\kappa_{ran}} = \frac{1}{3}\left(\frac{1}{\kappa_{\parallel}} + \frac{2}{\kappa_{\perp}}\right) \quad \text{(A-5)}$$

Slip Correction Factor and Adjusted Diameter. In the free molecular regime, from the gas kinetic theory, the drag forces can be expressed as[20]

$$F_d = -\pi\eta v\frac{L}{Kn}\left\{[(1 + (2\zeta)^{-1})]f + \left(2 - \frac{6 - \pi}{4}f\right)(\sin^2\theta + \zeta^{-1}\cos^2\theta)\right\}$$

$$= -\pi\eta v\frac{L}{Kn}G_{cylinder}(\zeta,\theta) \quad \text{(A-6)}$$

for a cylinder with flat ends, in which Kn = $2\lambda/D$, and f is the momentum accommodation factor, and as

$$F_d = -\pi\eta v\frac{a}{Kn}\left(\sin^2\theta\left\{A_p\left[4 + \left(\frac{\pi}{2} - 1\right)f\right] + \frac{C_p}{{B_p}^2}\left[2 + \frac{4{B_p}^2 + \pi - 6}{4}f\right]\right\} + \cos^2\theta\left\{2A_p f + \frac{C_p}{{B_p}^2}\left[{B_p}^2(4 - 2f) - 4 + \left(3 - \frac{\pi}{2}\zeta^{-2}\right)f\right]\right\}\right)$$

$$= -\pi\eta v\frac{a}{Kn}G_{spheroid}(\zeta,\theta) \quad \text{(A-7)}$$

for a prolate spheroid, in which Kn = λ/b, $A_p = (\sin^{-1} B_p)/B_p$, $B_p = \sqrt{1-\zeta^{-2}}$, and $C_p = \zeta^{-1} - A_p$.

The momentum accommodation factor can be obtained by[21]

$$f = \frac{1}{\pi}\left[\left(\frac{36\phi}{\alpha + \beta}\right) - 8\right] \quad \text{(A-8)}$$

The calculated value of the momentum accommodation factor in nitrogen gas, f, is 0.740 using $\phi = \eta/\rho_f\bar{c}\lambda$, in which ρf is the gas density, and $\bar{c}$ is the mean velocity of the gas molecules. The mean velocity of the gas molecules is obtained by $\bar{c} = 8R\sqrt{T}/\pi M$, in which R is the universal gas constant, M is the molecular weight of gas molecules, and T is the absolute temperature.

By equating eqs A-6, A-7, and 10, we obtain the adjusted spherical diameter of the spheroid and the cylindrical particle:

$$d_{a,cylinder} = \left(\frac{\alpha + \beta}{3}\right)\left(\frac{G_{cylinder}(\zeta,\theta)}{\kappa_{0,cylinder}(\theta)}\right)L\left(\frac{3\zeta}{2}\right)^{-1/3} \quad \text{(A-9)}$$

$$d_{a,spheroid} = \left(\frac{\alpha + \beta}{3}\right)\left(\frac{G_{spheroid}(\zeta,\theta)}{\kappa_{0,spheroid}(\theta)}\right)a\zeta^{-1/3} \quad \text{(A-10)}$$

With the volume-equivalent diameter of a cylinder ($d_{ve,cylinder} = D(3\zeta/2)^{1/3}$) and a spheroid ($d_{ve,spheroid} = 2b\zeta^{1/3}$), the mobility of nonspherical particles can be obtained using eq 3 and the drag coefficient given as eq 11, in which the slip correction factor is given as eq 12.

LA0513196

(20) Dahneke, B. E. *J. Aerosol Sci.* **1973**, *4*, 147−161.

(21) Allen, M. D.; Raabe, O. G. *J. Aerosol Sci.* **1982**, *13*, 537−547.